SCAPS numerical design of $MoSe_2$ solar cell for different buffer layers

T. A. Chowdhury *, R.B. Arif , H. Israq , N. Sharmili , R. S. Shuvo
Department of Electrical & Electronic Engineering, Ahsanullah University of Science & Technology, Dhaka, Bangladesh.

The solar cell capacitance simulator (SCAPS-1D) has been used to simulate, design and analyze of $MoSe_2$, an attractive transition metal dichalcogenide (TMDC) material, based heterojunction solar cells to use it as a potential alternative to conventional absorber layers used in solar cells. The work also focuses on finding optimal absorber, buffer layer thickness and impact of operating temperature on solar cell performance with a possible replacement to toxic CdS buffer layer. It has been obtained that the optimum thickness of $MoSe_2$ absorber layer is 1 µm and buffer layer is about 0.04 µm. The efficiency obtained with CdS based buffer layer solar cell is 20.21%. Among different buffer layers such as In_2S_3, ZnO, ZnOS and ZnSe, the highest efficiency obtained of $MoSe_2$ based solar cell is 20.58% with ZnO buffer layer. ZnO buffer based solar cell shows a temperature gradient of -0.355%/K compared to -0.347%/K for CdS buffer based solar cell. The findings of this work provide important guidance to fabricate high-efficiency $MoSe_2$ thin film solar cell with non-toxic ZnO as a potential buffer layer.

Received November 29, 2023; Accepted February 15, 2024)

Keywords: $MoSe_2$, Scaps-1D, Solar cell, Buffer layer, Temperature, Efficiency

1. Introduction

To meet the increasing energy crisis, promising alternative to fossil fuels can be photovoltaics (PV)[1-3]. A PV cell uses photovoltaic effect to convert the solar energy into electric current. Sustainability, renewability and cleanness are the features that cause solar energy conversion achieve a large attention globally in recent years [4]. Low-cost, high-efficient and developed deposition techniques are the various advantages that makes semiconducting absorber materials based thin-film solar cells potential candidates for photovoltaic device applications [5-10]. Intensive research is going on materials which can be applicable for thin film solar cells to obtain the maximum ratio efficiency/cost [11]. $Cu_2(In,Ga)Se_2$ (CIGS) and CdTe based solar cells have attained conversion efficiencies greater than 22% [12-13]. The drawback of thin-film solar cells based on these materials are expensive, toxic and rare elements [14-19]. To overcome the problem, new substitute materials $Cu_2ZnSn(S,Se)_4$ [20], $CuSbS_2$ [21], Sb_2S_3 [22-24] and Sb_2Se_3 [25-27] have been explored by researchers due to eco-friendly and low-cost features.

Recently, transition metal dichalcogenides (TMDCs) have obtained high attention due to their low-cost and superior thermal [28], mechanical [29], optical [30] and electrochemical properties [31,32]. TMDCs are used for various applications especially biomedical [33], batteries [34] and solar cells [35,36]. Low surface defect density of such materials makes them useful for optoelectronic applications [37-39]. TMDs such as MoS_2, $MoSe_2$, WS_2, WSe_2 etc. based solar cell are fabricated by chemical vapor deposition (CVD) and mechanical exfoliation methods [40, 41]. The advantage of TMDCs is that they are chemically and thermally stable with high carrier mobility, non-toxic, abundant, and cheap [42].

The $MoSe_2$ belongs to the group VI of the layered TMDCs. In the $MoSe_2$, the electronic structure of chalcogen Se is s^2p^4 and the transition metal Mo is $4d^25s^2$ i.e. two electrons are missing for a filled shell for both elements [43]. Their structure is composed of X-M-X planes where for the in-plane sheets two chalcogen layers sandwiches a layer of metal atoms with a strong covalent bonding and the sheets are held by a weak Van der Waals coupling [42,44-46].

* Corresponding author: towhid6789@yahoo.com
https://doi.org/10.15251/CL.2024.212.175

Bulk $MoSe_2$ has indirect band gap. Thin $MoSe_2$ monolayer has a direct band gap of 1.6 eV and high electron mobility of 100 $cm^2V^{-1}s^{-1}$ that makes them a potential candidate for thin film solar cells [47-49]. There is lack of simulation reports that have proven application of MoSe2 thin films as absorber layer in solar cells.

In this work, novel inorganic hetero-junction $MoSe_2$ based thin film solar cells are simulated using the solar cell capacitance simulator (SCAPS-1D) software with different buffer layers. The impact of absorber and buffer layer thickness and operating temperatures on solar cell fundamental parameters such as open circuit voltage (V_{OC}), short-circuit current density (J_{SC}), fill factor (FF) and efficiency (η) are studied and optimized to obtain the maximum efficiency of proposed solar cell.

2. Simulation methodology and device structure

Numerical simulation is a valuable approach to investigate the performance parameters of a solar cell by varying input parameters and thus to predict the performance of the cell with quick time and low-cost. In this present work, design and simulation of thin film solar cell based on $MoSe_2$ absorber layer is carried out by SCAPS-1D software developed by University of Gent, Belgium [50]. SCAPS uses Poisson's and continuity equations for electrons and holes to provide results [51-54]. The current–voltage (I–V) characteristics in the dark and under illumination, capacitance–voltage (C–V) characteristics, external quantum efficiency (EQE), electric field distributions, energy bands of materials used in the solar cell and recombination profile of the solar cells can be explored using the SCAPS-1D simulator. These may be studied as a function of temperature. In the present work, impact of absorber, buffer layer thickness and operating temperature on $MoSe_2$ based solar cell with different buffer layer are investigated and optimized with a view to find replacement of conventional toxic CdS.

Fig. 1 shows the schematic structure of the Mo / $MoSe_2$ / Buffer layer / FTO solar cell where $MoSe_2$ is used as p-type absorbent layer, the CdS, InS, ZnO, ZnOS and ZnSe as the different n-type buffer layers in our simulation. Mo plays the role of back contact and fluorine-doped tin oxide (FTO) as the window layer. The parameters used in our simulations are summarized in Table I. The device is irradiated with AM 1.5G spectrum with the incident power density of 1000 W/m^2 at a room temperature of 300 K.

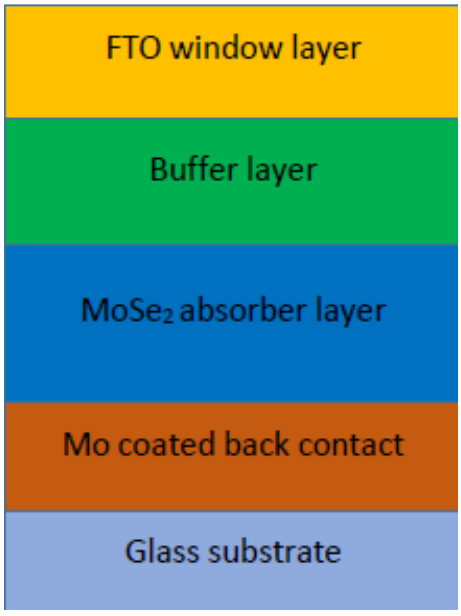

Fig. 1. Schematic diagram of $MoSe_2$ solar cell.

Table 1. Physical parameters of different layers used for the simulation.

Parameter	$MoSe_2$	CdS	In_2S_3	ZnO	ZnOS	ZnSe	FTO
Thickness(μm)	0.5-5	0.01-0.1	0.01-0.1	0.01-0.1	0.01-0.1	0.01-0.1	0.1
Band gap (eV)	1.45	2.4	2.8	3.3	2.83	2.9	3.6
Electron affinity (eV)	4.05	4.4	4.5	4	3.6	4.1	4.0
Dielectric permittivity	11.9	10	13.5	9	9	10	9
CB effective density of states (cm^{-3})	2.8×10^{19}	2.2×10^{18}	2.2×10^{17}	3.7×10^{18}	2.2×10^{18}	1.5×10^{18}	2.2×10^{18}
VB effective density of states (cm^{-3})	2.65×10^{19}	1.8×10^{19}	1.8×10^{19}	1.8×10^{19}	1.8×10^{18}	1.8×10^{18}	1.8×10^{19}
Electron thermal velocity (cms^{-1})	1×10^7	1×10^7	1×10^7	1×10^7	1×10^7	1×10^7	1×10^7
Hole thermal velocity (cm^{-1})	1×10^7	1×10^7	1×10^7	1×10^7	1×10^7	1×10^7	1×10^7
Electron mobility (cm^2/Vs)	1450	100	100	100	100	50	100
Hole mobility(cm^2/Vs)	50	25	25	25	25	20	25
Shallow uniform donor density, N_D (cm^{-3})	0	1×10^{17}	1×10^{17}	1×10^{17}	1×10^{18}	1×10^{17}	1×10^{19}
Shallow uniform acceptor density, N_A (cm^{-3})	1×10^{16}	0	0	0	0	0	0

3. Results and discussion

3.1. Effect of $MoSe_2$ absorber layer's thickness

To study the impact of absorber layer thickness on cell performance, the thickness of $MoSe_2$ layer is varied from 0.5 to 5 μm for CdS/$MoSe_2$ solar cell using SCAPS while all other input parameters is kept constant. The thickness of CdS buffer layer is considered 0.05 μm for the simulation. Fig. 2 shows the device performance parameters with variable thickness of $MoSe_2$ absorber layer. If absorber layer thickness is too thin, efficiency is low due to an inadequate absorption of the incident photons with higher recombination rate at the back contact of photo-generated carriers as depletion region is closer [51,55]. As thickness is increased, most of the photons of long wavelengths will be collected and the absorber layer will generate more electron-hole pairs which increases efficiency [56]. However, when the absorber layer is too thick, the generated electron–hole pairs may recombine before arriving at the charge accumulating metal contact and being collected [57,58]. As a result, the solar cell efficiency cannot be enhanced significantly.

It is observed that when the thickness of the absorber layer increases from 0.5 to 1 μm, V_{oc} increases from 0.818 V to 0.822 V (an increment about 0.49%), J_{SC} increases from 27.1 mA/cm^2 to 29.2 mA/cm^2(an increment about 7.75%), and η increases from 18.66% to 20.19% (an increment about 8.2%). For the increment of absorber layer thickness from 1 to 1.5 μm, V_{oc} increases to from 0.822 V to 0.825 V (an increment about 0.36%), J_{SC} increases from 29.2 mA/cm^2 to 29.59 mA/cm^2 (an increment about 1.33%), and η increases from 20.19% to 20.6% (an increment about 2.03%). So the increase of these parameters occur at a slow rate for increase of absorber layer thickness of 0.5 μm from 1 to 1.5 μm. If absorber layer thickness is further increased, all the parameters increase at a much slower rate. The highest efficiency achieved is 21.4% for absorber layer

thickness of 5 μm. To decrease the usage of $MoSe_2$ thickness and deposition time, the optimal $MoSe_2$ absorber layer thickness selected is 1 μm for the simulation.

The spectral response of $MoSe_2$ based solar cell for different absorber layer thickness is shown in Fig. 3. The maximum quantum efficiency (QE) of 1 is obtained if each photon produces a pair electron-hole for a given wavelength. With increase in absorber layer thickness, more photons of long wavelengths are absorbed which results in increase in electron–hole pairs production. As a result, with increase in absorber layer thickness, QE is improved. For absorber layer thickness less than 1 μm, due to the light transmission lowest quantum efficiency is obtained in the 550–860 nm wavelength range [59]. Quantum efficiency (QE) above 90% is gained with absorber layer thickness greater or equal to 1 μm for the 550–860 nm wavelength range. The quantum efficiency is negligible for wavelengths greater than 860 nm due to light not being absorbed below band gaps at long wavelengths of low-energy photons [60]. The results indicate that when the absorber layer thickness is increased more photons are absorbed.

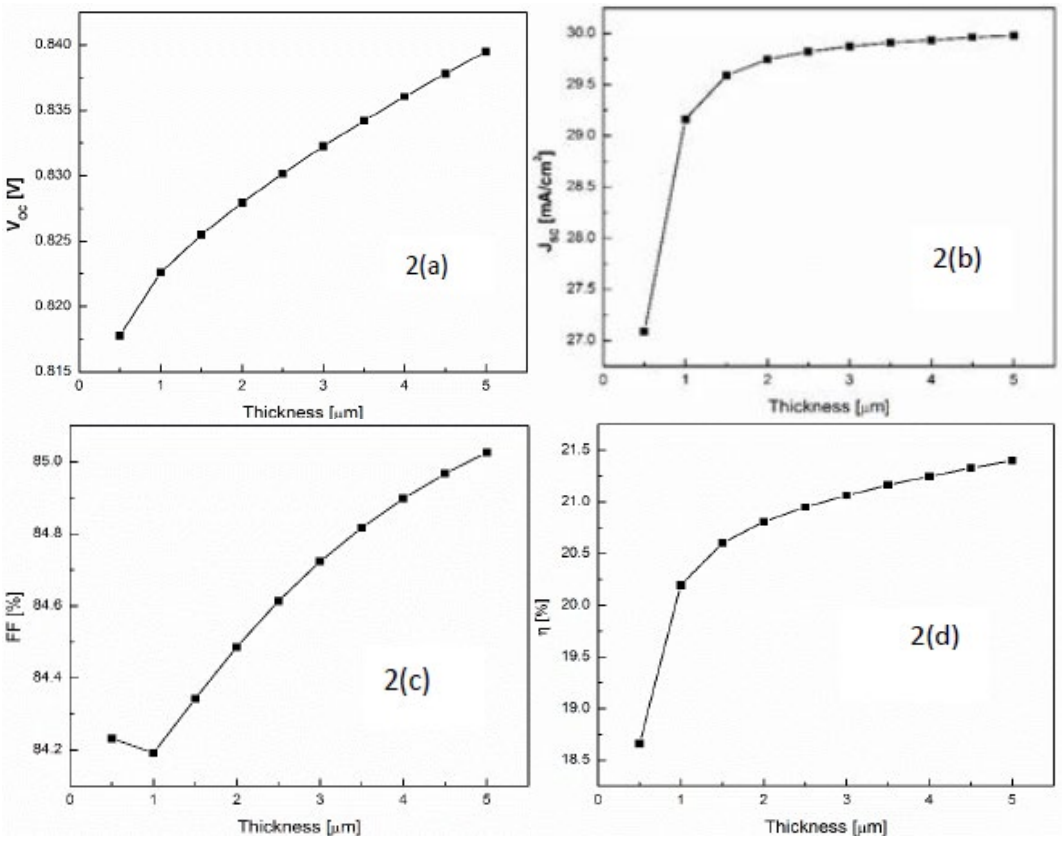

Fig. 2. a V_{oc} vs. absorber layer thickness. b J_{sc} vs. absorber layer thickness. c Fill factor vs. absorber layer thickness. d Efficiency vs. absorber layer thickness

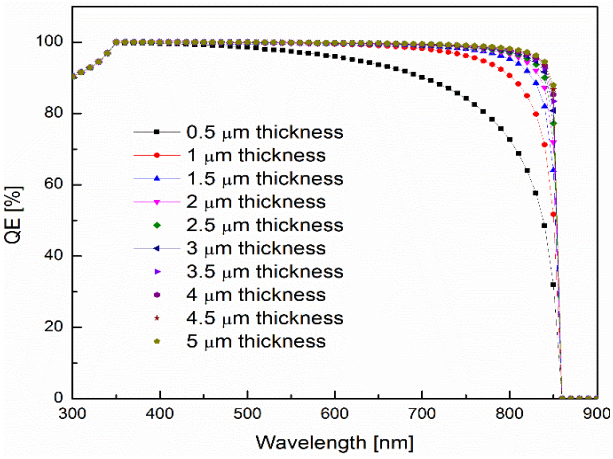

Fig. 3. Spectral response for different $MoSe_2$ absorber layer thicknesses.

3.2. Effect of CdS buffer layer thickness

The CdS layer thickness was varied from 0.01 to 0.1 μm with a fixed $MoSe_2$ absorber layer thickness of 1 μm in this simulation. The impact of change in CdS buffer layer thickness is shown in Fig. 4. V_{oc} and J_{sc} is almost unaffected by the variation of buffer layer thickness. FF decreases nonlinearly from 85% to 84.26% as buffer layer thickness is increased from 0.01 to 0.04 μm as series resistance increases [55]. Beyond 0.05 μm of buffer layer thickness, FF is almost constant around 84.16%. The combined effect of $V_{oc,}$ J_{sc} and FF causes η to decrease from 20.4% to 20.21% as buffer layer thickness is increased from 0.01 to 0.04 μm. If buffer layer thickness is increased in the range 0.05-0.1 μm, η value saturates around 20.19%. The decrease in FF mainly causes the efficiency to decrease. The results indicate that efficiency decrease with increase in buffer layer thickness. Leakage current may flow if buffer layer is too thin. The increase in thickness of the buffer layer enhances recombination rate as the photo-generated carriers need to travel longer distances than their diffusion lengths to reach front contact. As a result, efficiency of solar cell decreases [15]. Due to the difficulty to fabricate high-quality CdS films too thin (< 0.03 μm) practically, and the reason that the thick buffer layers reduce the solar cell efficiency, the optimum buffer thickness would be from 0.03 μm to 0.05 μm. For this simulation, the optimal CdS buffer layer thickness selected is 0.04 μm which results in efficiency of 20.21%.

Fig. 5 shows spectral response of $MoSe_2$ based solar cells with variable thickness of CdS buffer layer.With increase in buffer layer thickness, more incident photons is captured into the buffer layer, and the absorber layer will capture fewer photons [61]. As a result, there is reduction in quantum efficiency as less amount of electron-hole pairs are generated by absorber layer. For small thickness of CdS buffer layer, electron-hole pairs generated by short wavelength photons can be collected by contacts before they can recombine as their diffusion lengths are adequate [15]. For different buffer layer thickness, QE has the same behavior as buffer layer bandgap is higher than incident photons energy in 350-860 nm wavelength range. QE above 90% is obtained in this wavelength range. QE is lower in 300-350 nm wavelength range due to absorption in the buffer layer. Buffer layer bandgap is lower than incident photons in this wavelength range which causes absorption. Less photons are able to transmit to the absorber layer due to increase in parasitic absorption in buffer layer with increase in buffer layer thickness [59,62]. There is no significant impact on QE behavior for variation of CdS buffer layer thickness in considered range 0.01-0.1 μm in this simulation.

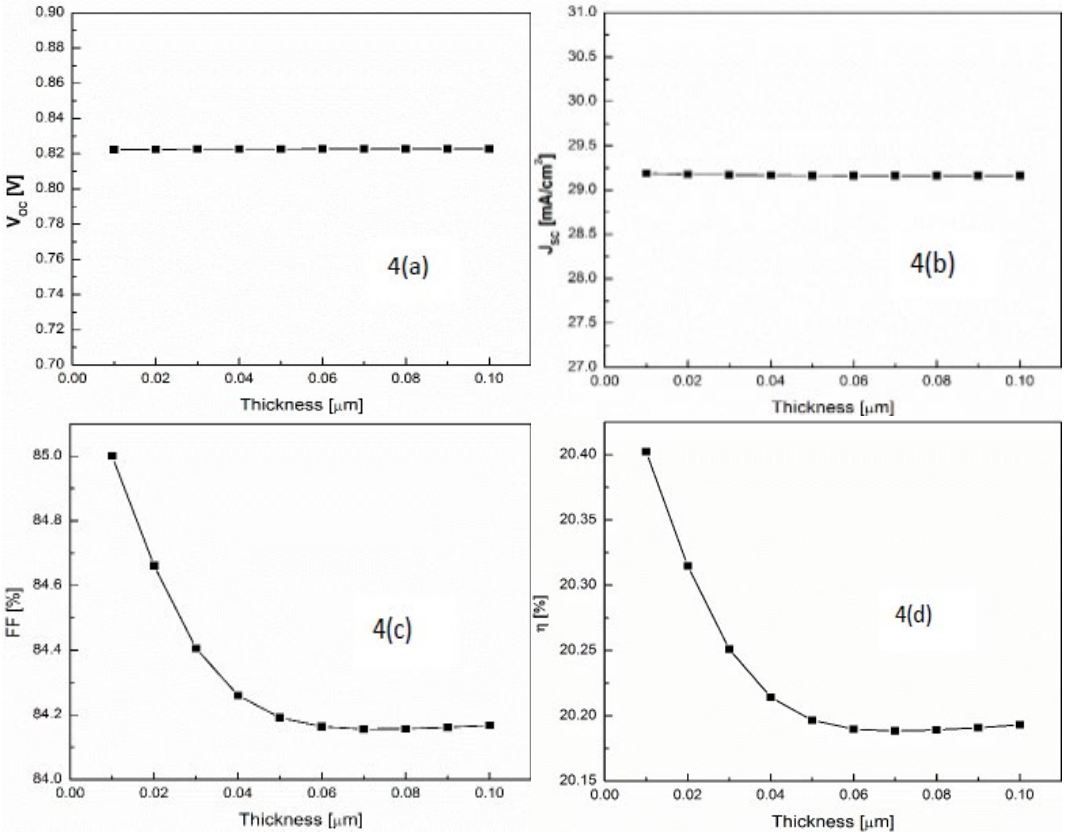

Fig. 4. a V_{oc} vs. buffer layer thickness. b J_{sc} vs. buffer layer thickness. c Fill factor vs. buffer layer thickness. d Efficiency vs. buffer layer thickness.

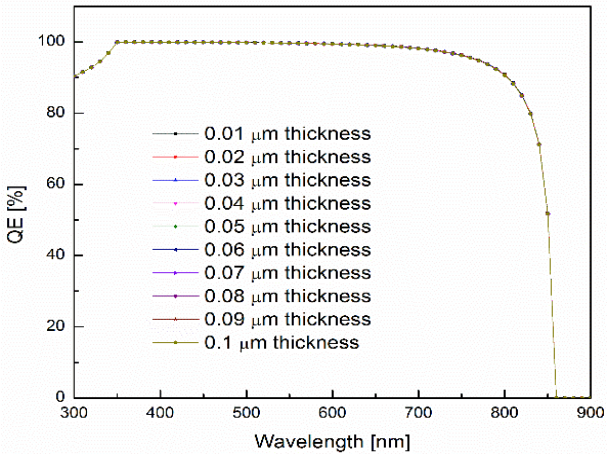

Fig. 5. Spectral response of SnS based solar cell with variable thickness of CdS buffer layer.

3.3. Effect of different buffer layers on cell performance

P-N junction is created with the p-type absorber layer with the help of n-type buffer layer. The large bandgap of buffer layer compared to the absorber layer allows most light to travel to the junction region. This causes increased electron-hole pair generation via photon absorption [61,63,64]. Band alignment between the absorber and window layer is provided by buffer layer and it also decreases interfacial strain and defects caused by the window layer [65,66]. CdS has optical gap of 2.45 eV and covers 24% of solar spectrum by absorbing photons below 590 nm wavelength [67]. This property makes CdS a promising buffer layer. The main drawback is

toxicity of Cd. To overcome this issue, other non-toxic and wide bandgap potential buffer layers such as In_2S_3, ZnO, ZnOS and ZnSe have been investigated while keeping thickness of $MoSe_2$ absorber layer fixed at 1 µm. The buffer layer thickness used is 0.04 µm for all buffer layers in this simulation which is the optimal buffer layer thickness obtained for CdS using $MoSe_2$ absorber layer in previous section. Figure 6 shows the electrical parameters (V_{oc}, J_{sc}, FF and η) for different buffer layers of $MoSe_2$ based solar cell as obtained from the simulation. The current density–voltage (J–V) and spectral response for different buffer layers are shown in Fig. 7 and Fig. 8 respectively. V_{OC} is almost unaffected by different buffer layer with value around 0.822 V. J_{SC} with CdS, In_2S_3, ZnO, ZnOS and ZnSe as buffer layer is 29.17 mA/cm^2, 29.16 mA/cm^2, 29.22 mA/cm^2, 29.23 mA/cm^2 and 29.22 mA/cm^2 respectively. FF with CdS, In_2S_3, ZnO, ZnOS and ZnSe as buffer layer is 84.26%, 77.98%, 85.67%, 81.47% and 85.64% respectively. $MoSe_2$ based solar cell with ZnOS buffer layer has low QE compared to other buffer layers. $MoSe_2$ based solar cell with CdS, In_2S_3, ZnO, ZnOS and ZnSe as buffer layers results in efficiency of 20.21%,18.73%, 20.58%, 19.58% and 20.57 %, respectively in the simulation. FF is the main reason for difference in efficiency for different buffer layer. Hence, ZnO and ZnSe are highly prospective alternative to CdS buffer layer in $MoSe_2$ based solar cell as they obtain efficiency above 20.21% and have wider bandgap than CdS. The highest efficiency obtained is with ZnO buffer layer.

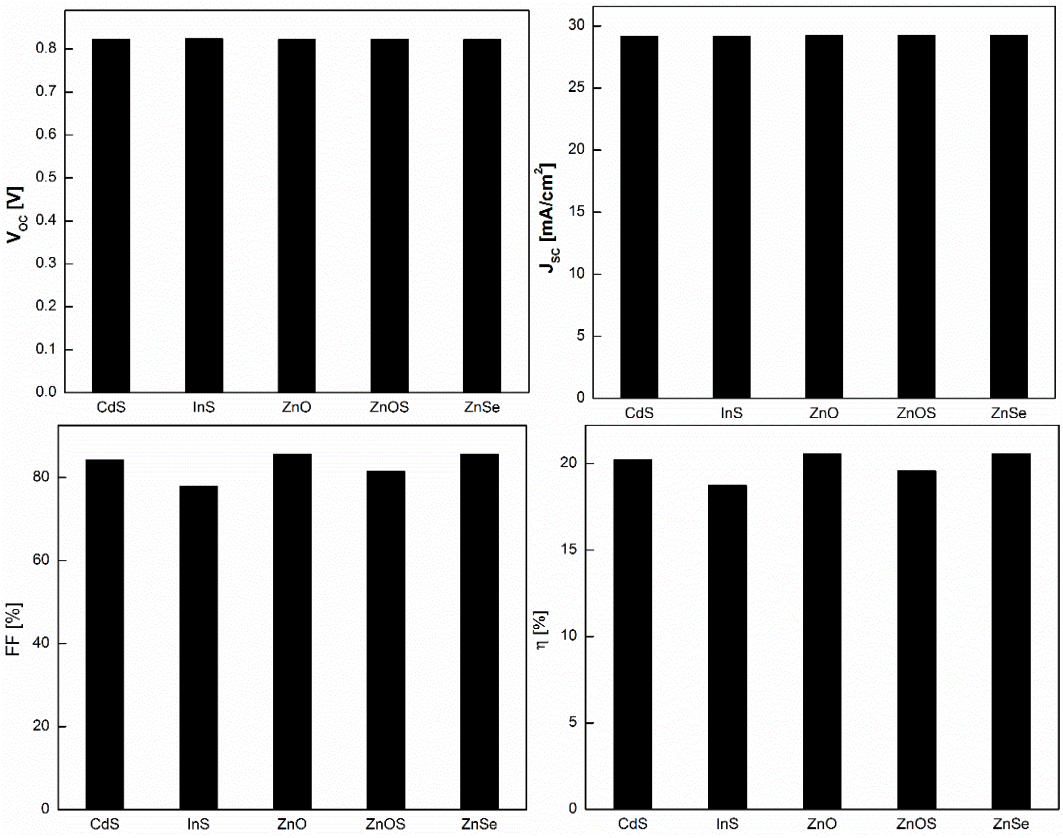

Fig. 6. $MoSe_2$ based solar cell performance with different buffer layer.

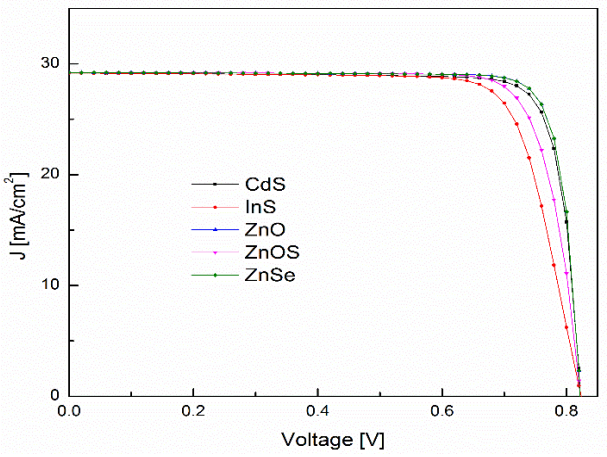

Fig. 7. J–V characteristics of $MoSe_2$ based solar cell with different buffer layer.

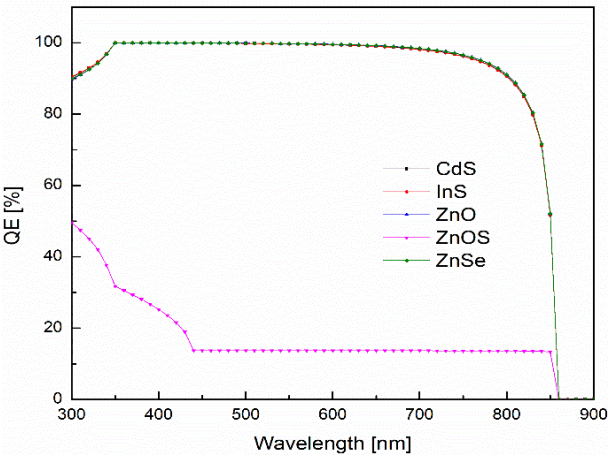

Fig. 8. Spectral response of $MoSe_2$ based solar cell with different buffer layers

3.4. Effects of operating temperature with various buffer layer

The sunlight will increase the temperature of solar panels as they are installed outdoor. So the impact of temperature is analyzed for $MoSe_2$ based solar cell with various buffer layers in temperature range of 300 K to 400 K as temperature plays a major role in solar cell performance. The optimal $MoSe_2$ absorber layer's thickness of 1 µm, while the buffer layer's thickness of 0.04 µm as obtained in previous section is used for simulation of proposed solar cell with different buffer layer. Figure 9 presents the impact of temperature on $MoSe_2$ solar cell performance parameters with different buffer layers. V_{OC} decreases and J_{SC} increases slightly with increase in temperature for all buffer layers used in simulation. FF for CdS, ZnO and ZnSe buffer layer decreases with increase in temperature. For In_2S_3 and ZnOS buffer layer FF increases with temperature upto 340 K and 320 K respectively due to decrease in series resistance. Then FF decreases for both buffer layers with increase in temperature upto 400 K. The combined effect of V_{OC}, J_{SC} and FF causes efficiency to degrade with increase in temperature. The efficiency with CdS, In_2S_3, ZnO, ZnOS and ZnSe as buffer layer for $MoSe_2$ based solar cell decrease from 20.21% to 13.2%, 18.73% to 13.12%, 20.58% to 13.27%,19.58% to 13.26% and 20.57% to 13.26% respectively as temperature is increased from 300 K to 400 K.

With increase in temperature, the mobility of carriers decreases as their number increase. This causes reverse saturation current to increase which results in decrease in V_{OC} [59]. Adequate energy is gained by more photons to generate electron-hole pairs as bandgap energy of material is decreased with increase in temperature. This causes J_{SC} to increase with rise in temperature [68-

70]. Phonons activated with increase in temperature enhance the scattering rate of charge carriers which impacts material conductivity. As a result, solar cell conversion efficiency decreases with increase of temperature [71].

To understand their stability, the temperature degradation gradients have been analyzed for $MoSe_2$ based solar cell structures with different buffer layers. Figure 10 presents the impact of temperature on normalized efficiency of $MoSe_2$ solar cells with different buffer layers. The declination of efficiency with CdS buffer layer solar cell with temperature is -0.347%/K. For non-toxic Cd-free buffer layers used in the simulation such as In_2S_3, ZnO, ZnOS and ZnSe the efficiency decreases with temperature gradient of -0.299%/K, -0.355%/K, -0.323%/K and -0.355%/K respectively with increase in temperature. So, it is observed that all solar cell structures with different buffer layers perform better at low room temperature.

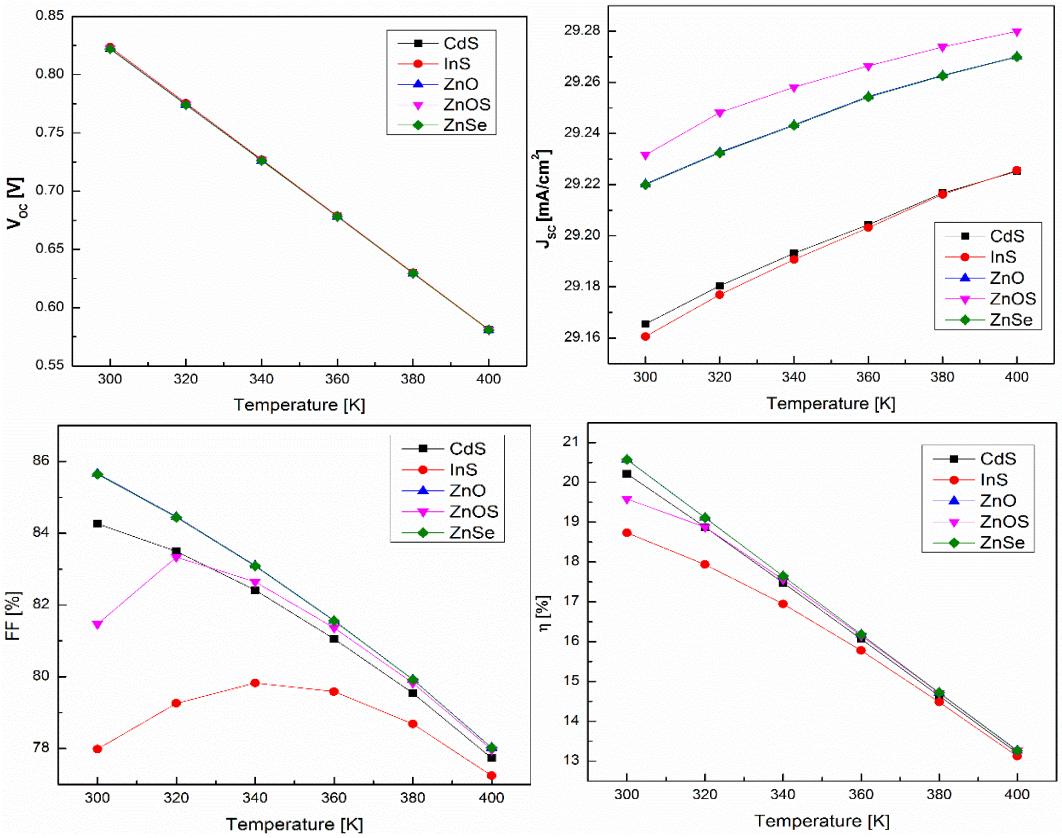

Fig. 9. Effect of temperature on performance of $MoSe_2$ based solar cell with different buffer layers.

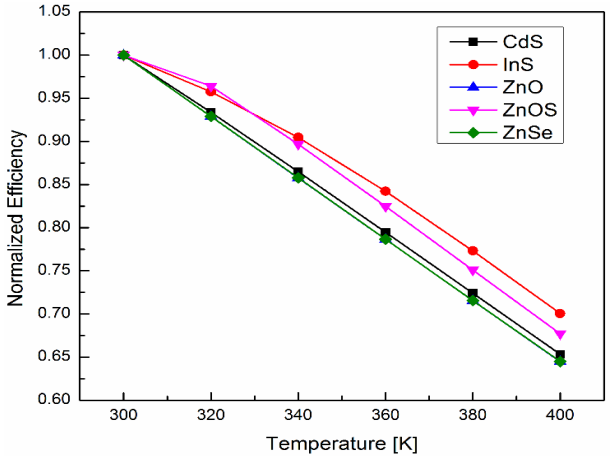

Fig. 10. Effect of temperature on normalized efficiency of $MoSe_2$ based solar cell with different buffer layers.

4. Conclusions

In this study, photovoltaic performance of heterojunction solar cells based on $MoSe_2$, a transition-metal dichalcogenide, have been numerically analysed with five different buffer layers such as CdS, In_2S_3, ZnO, ZnOS and ZnSe using the SCAPS 1-D software. The impact of CZTS absorber, buffer layer thickness and operating temperature on the solar cell performance is investigated. The main focus is to obtain a non-toxic Cd-free potential buffer layer with optimal absorber and buffer layer thickness. The optimal thickness of $MoSe_2$ absorber layer and buffer layer found is 1 µm and 0.04 µm respectively. The highest efficiency obtained of $MoSe_2$ based solar cell with ZnO buffer layer is 20.58% (Jsc = 29.22 mA/cm^2, Voc = 0.822 V and FF = 85.67%). The temperature gradient with CdS, In_2S_3, ZnO, ZnOS and ZnSe buffer layer found is -0.347%/K, -0.299%/K,-0.355%/K, -0.323%/K and -0.355%/K respectively with increase in temperature. So solar cell performance with different buffer layers degrades with increase in temperature. ZnO is a promising alternative to toxic CdS buffer layer in $MoSe_2$ based solar cell based on simulation results obtained. So the design configuration will be helpful to fabricate low-cost, non-toxic and high-efficient $MoSe_2$ absorber layer based solar cell as simulation results obtained are comparable with other existing thin film solar cells.

Acknowledgements

The author acknowledges Dr. Marc Burgelman and his colleagues at the University of Gent, Belgium, for providing SCAPS 1-D simulation program.

References

[1] N. T. Kalyani, S.J. Dhoble, Nanomaterials for Green Energy , 325 (2018).

[2] S. Ahmmed, A. Aktar, S. Tabassum, M. H. Rahman, M. F. Rahman, A. B. M. Ismail, Superlattices and Microstructures, 151, 106830 (2021); https://doi.org/10.1016/j.spmi.2021.106830

[3] J.M. Pearce, Futures, 34, 663 (2002); https://doi.org/10.1016/S0016-3287(02)00008-3

[4] A. Khadir, Acta Physica Polonica A ,137,1128 (2020); https://doi.org/10.12693/APhysPolA.137.1128

[5] M. Nakamura, K. Yamaguchi, Y. Kimoto, Y. Yasaki , T. Kato , H. Sugimoto, IEEE Journal of Photovoltaics, 9, 1863 (2019); https://doi.org/10.1109/JPHOTOV.2019.2937218

[6] A. Hu., J. Zhou, P. Zhong, X. Qin , M. Zhang, Y. Jiang, X. Wu, D. Yang, Solar Energy, 214, 319 (2021); https://doi.org/10.1016/j.solener.2020.12.008

[7] M. Powalla, S. Paetel, E. Ahlswede, R. Wuerz, C.D. Wessendorf, T.M. Friedlmeier, Applied Physics Reviews, 5 ,041602 (2018); https://doi.org/10.1063/1.5061809

[8] M.A. Green, Y. Hishikawa, E.D. Dunlop, D.H. Levi, J.H. Ebinger, A.W.Y. Ho-Baillie, Progress in Photovoltaics: Research and Applications, 26 ,427 (2018).

[9] C.T. Lee, K.F. Lu, C.Y. Tseng, Solar Energy ,114, 1 (2015); https://doi.org/10.1016/j.solener.2015.01.023

[10] N.R. Paudel, K.A.Wieland, A.D. Compaan, Solar Energy Materials and Solar Cells , 105, 109 (2012); https://doi.org/10.1016/j.solmat.2012.05.035

[11] H. Heriche , Z. Rouabah , N. Bouarissa, International Journal of Hydrogen Energy, 42, 9524 (2017); https://doi.org/10.1016/j.ijhydene.2017.02.099

[12] M.A. Green, E.D. Dunlop, G. Siefer, M. Yoshita, N. Kopidakis, K. Bothe,X. Hao, Progress in Photovoltaics: Research and Applications, 31, 3 (2023); https://doi.org/10.1002/pip.3646

[13] A. Khadir, Acta Physica Polonica A ,144, 52 (2023); https://doi.org/10.12693/APhysPolA.144.52

[14] M. Jamil, M. Amami, A. Ali, K. Mahmood, N. Amin, Solar Energy, 231, 41 (2022); https://doi.org/10.1016/j.solener.2021.11.025

[15] W. Hennia, W.L. Rahal, D. Rached, Acta Physica Polonica A , 142, 445 (2022); https://doi.org/10.12693/APhysPolA.142.445

[16] X.X. Wu, Solar Energy, 77, 803 (2004); https://doi.org/10.1016/j.solener.2004.06.006

[17] P. Jackson, D. Hariskos, E. Lotter, S. Paetel, R. Wuerz, R. Menner, W. Wischmann, M. Powalla, Progress in Photovoltaics: Research and Applications, 19, 894 (2011); https://doi.org/10.1002/pip.1078

[18] M.A. Green, Progress in Photovoltaics: Research and Applications, 14, 383 (2006); https://doi.org/10.1002/pip.702

[19] B.A. Andersson, C. Azar, J. Holmberg, S. Karlsson, Energy, 23, 407 (1998); https://doi.org/10.1016/S0360-5442(97)00102-3

[20] W. Wang, M.T. Winkler, O. Gunawan, T.Gokmen, T.K. Todorov, Y. Zhu ,D.B. Mitzi, Advanced Energy Materials, 4,1301465 (2014); https://doi.org/10.1002/aenm.201301465

[21] W. Septina, S. Ikeda, Y. Iga, T. Harada, M. Matsumura, Thin Solid Films, 550 ,700 (2014); https://doi.org/10.1016/j.tsf.2013.11.046

[22] R. Tang, X. Wang, C. Jiang, S. Li, G. Jiang, S. Yang, C. Zhu ,T. Chen, Journal of Materials Chemistry A, 6,16322 (2018); https://doi.org/10.1039/C8TA05614E

[23] P. Myagmarsereejid, M. Ingram, M. Batmunkh, Y.L. Zhong, Nano-Micro Small, 17, 2100241 (2021); https://doi.org/10.1002/smll.202100241

[24] R. Kondrotas, C. Chen, J. Tang, Joule, 2, 857 (2018); https://doi.org/10.1016/j.joule.2018.04.003

[25] R. Tang, Z.-H. Zheng, Z.-H. Su, X.-J. Li, Y.-D. Wei, X.-H. Zhang, Y.-Q. Fu, J.-T. Luo, P. Fan, G.-X. Liang, Nano Energy, 64 ,103929 (2019); https://doi.org/10.1016/j.nanoen.2019.103929

[26] A. Khadir, Optical Materials, 127, 112281 (2022); https://doi.org/10.1016/j.optmat.2022.112281

[27] R. Tang, S. Chen, Z.H. Zheng, Z.H. Su, J.T. Luo, P. Fan, X.H. Zhang, J. Tang, G.X. Liang, Advanced Materials, 34, 2109078 (2022); https://doi.org/10.1002/adma.202109078

[28] C. Chiritescu, D.G. Cahill, N. Nguyen, D. Johnson, A. Bodapati, P. Keblinski, P. Zschack, Science, 315, 351 (2007); https://doi.org/10.1126/science.1136494

[29] S. Dominguez-Meister, A. Justo, J. C.Sanchez-Lopez, Materials Chemistry and Physics, 142, 186 (2013); https://doi.org/10.1016/j.matchemphys.2013.07.004

[30] W. Zhao, R.M. Ribeiro, M. Toh, A. Carvalho, C. Kloc, A.H.C. Neto, G. Eda, Nano Letters, 13, 5627 (2013); https://doi.org/10.1021/nl403270k

[31] M.A. Lukowski, A.S. Daniel, C.R. English, F. Meng, A. Forticaux, R.J. Hamers, S. Jin, Energy & Environmental Science, 7, 2608 (2014); https://doi.org/10.1039/C4EE01329H

[32] S.T. Finn, J.E. Macdonald, ACS Applied Materials & Interfaces, 8, 25185 (2016); https://doi.org/10.1021/acsami.6b05101

[33] S. Anju, P.V. Mohanan, Synthetic Metals, 271, 116610 (2021); https://doi.org/10.1016/j.synthmet.2020.116610

[34] B. Chen, D. Chao,E. Liu, M. Jaroniec, N. Zhao, S.-Z. Qiao, Energy & Environmental Science, 13, 1096 (2020); https://doi.org/10.1039/C9EE03549D

[35] M. Moustafa, T.A. Zoubi, S.Yasin, Optical Materials, 124, 112001 (2022); https://doi.org/10.1016/j.optmat.2022.112001

[36] L. Li, H. Wang, X. Fang, T. Zhai, Y. Bando , D. Golberg, Energy & Environmental Science, 4, 2586 (2011); https://doi.org/10.1039/c1ee01286j

[37] W. Jaegermann, H. Tributsch, Progress in Surface Science, 29 ,1 (1988); https://doi.org/10.1016/0079-6816(88)90015-9

[38] A. Klein, Y. Tomm, R. Schlaf, C. Pettenkofer, W. Jaegermann, M. Lux-Steiner, E. Bucher, Solar Energy Materials and Solar Cells, 51, 181 (1998); https://doi.org/10.1016/S0927-0248(97)00234-1

[39] M. A. Rahman, Heliyon, 8, e09800 (2022); https://doi.org/10.1016/j.heliyon.2022.e09800
[40] T. Akama, W. Okita, R. Nagai, C. Li, T. Kaneko, T. Kato, Scientific Reports, 7, 11967 (2017); https://doi.org/10.1038/s41598-017-12287-6
[41] E. Singh, K.S. Kim, G.Y. Yeom, H.S. Nalwa, RSC Advances,7, 28234 (2017); https://doi.org/10.1039/C7RA03599C
[42] M. Moustafa, T. Al Zoubi, S. Yasin, Brazilian Journal of Physics,52, 141 (2022); https://doi.org/10.1007/s13538-022-01146-z
[43] T. Alzoubi ,M. Moustafa, Modern Physics Letters B, 2050065 (2019); https://doi.org/10.1142/S0217984920500657
[44] M. Moustafa, A. Ghafari, A. Paulheim, C. Janowitz, R. Manzke, Journal of Electron Spectroscopy and Related Phenomena, 189, 35 (2013); https://doi.org/10.1016/j.elspec.2012.12.010
[45] M. Moustafa, A. Paulheim, M. Mohamed, C. Janowitz, R. Manzke, Applied Surface Science, 366, 397 (2016); https://doi.org/10.1016/j.apsusc.2016.01.024
[46] M. Elbar, S. Tobbeche, Energy Procedia, 74, 1220 (2015); https://doi.org/10.1016/j.egypro.2015.07.766
[47] Y. Shi, C. Hua, B. Li et al., Advanced Functional Materials, 23, 1832 (2013); https://doi.org/10.1002/adfm.201202144
[48] J. Tao, J. Chai, X. Lu, L. M. Wong, T. I. Wong, J. Pan, Q. Xiong, D. Chi, S. Wang, Nanoscale, 7, 2497 (2015); https://doi.org/10.1039/C4NR06411A
[49] B. Zaidi, C. Shekhar, B. Hadjoudja, S. Gagui, B. Chouial, Acta Physica Polonica A, 136, 495 (2019); https://doi.org/10.12693/APhysPolA.136.495
[50] M. Burgelmann, P. Nollet, S. Degrave, Thin Solid Films, 361-362, 527 (2000); https://doi.org/10.1016/S0040-6090(99)00825-1
[51] M. Burgelman, J. Verschraegen, S. Degrave, P. Nollet, Progress in Photovoltaics: Research and Applications , 12, 143 (2004); https://doi.org/10.1002/pip.524
[52] J. Verschraegen, M. Burgelman, Thin Solid Films, 515, 6276 (2007); https://doi.org/10.1016/j.tsf.2006.12.049
[53] K. Decock, S. Khelifi, M. Burgelman, Thin Solid Films, 519, 7481 (2011); https://doi.org/10.1016/j.tsf.2010.12.039
[54] N. Alhuda, Q. Algwari, Solid State Technology, 63, 1703 (2020).
[55] H. Elfarri, M. Bouachria, A. Frimanea, M. Fahoumea, O. Daoudia, M. Battas, Chalcogenide Letters, 18 (4), 201 (2021); https://doi.org/10.15251/CL.2021.184.201
[56] P. Chelvanathan, M, I. Hossain, N. Amin,Current Applied Physics, 10, S387 (2010); https://doi.org/10.1016/j.cap.2010.02.018
[57] K. K. Subedi, A. Phillips, N. Shrestha, F.K. Alfadhili, A. Osella, I. Subedi, R.A. Awni, E. Bastola, Z. Song, D. Li, R.W. Collins, Y. Yan, N. Podraza, M. Heben, R. Ellingson, Nano Energy, 83, 105827 (2021); https://doi.org/10.1016/j.nanoen.2021.105827
[58] M. I. Hossain, P. Chelvanathan, M. Zaman, M. R. Karim, M. A. Alghoul, N. Amin, Chalcogenide Letters, 8, 315 (2011).
[59] J. C. Z. Medina, E. R. Andres , C. M. Ruiz, E. C. Espinosa, L. T. Yarce , R. G. Isasmendi , R. R. Trujillo , G. G. Salgado , A. C. Solis , F. G. N. Caballero, A. C. C. Sanchez, Heliyon, 9, e14547, (2023); https://doi.org/10.1016/j.heliyon.2023.e14547
[60] A. Sunny, S. Rahman, M. M. Khatun, S. R. A. Ahmed, AIP Advances, 11, 065102 (2021); https://doi.org/10.1063/5.0049646
[61] O.K. Simya, A. Mahaboobbatcha, K. Balachander, Superlattices and Microstructures,82, 248 (2015); https://doi.org/10.1016/j.spmi.2015.02.020
[62] X. He, Y. Song, L. Wu, C. Li , J. Zhang, L. Feng, Materials Research Express, 5, 065907 (2018); https://doi.org/10.1088/2053-1591/aacae2
[63] A. A. Abdelkadir, E. Oublal, M. Sahal, A. Gibaud, Results in Optics, 8, 100257 (2022); https://doi.org/10.1016/j.rio.2022.100257

[64] O.K. Simya, A. Mahaboobbatcha, K. Balachander, Superlattices and Microstructures, 92, 285 (2016); https://doi.org/10.1016/j.spmi.2016.02.019

[65] F. A. Jhuma, M. Z. Shaily, M. J. Rashid, Materials for Renewable and Sustainable Energy, 8, 6 (2019); https://doi.org/10.1007/s40243-019-0144-1

[66] W. Eisele, A. Ennaoui, P. Schubert-Bischoff, M. Giersig, C. Pettenkofer, J. Krauser, M. Lux-Steiner, S. Zweigart, F. Karg, Solar Energy Materials and Solar Cells, 75, 17 (2003); https://doi.org/10.1016/S0927-0248(02)00104-6

[67] M. Nguyen, K. Ernits, K.F. Tai, C.F. Ng, S.S. Pramana, W.A. Sasangka, S.K. Batabyal, T. Holopainen, D. Meissner, A. Neisser, L.H. Wong, Solar Energy, 111, 344 (2015); https://doi.org/10.1016/j.solener.2014.11.006

[68] M.A. Green, Progress in Photovoltaics: Research and Applications, 11, 333 (2003); https://doi.org/10.1002/pip.496

[69] P. Singh, N.M. Ravindra, Solar Energy Materials and Solar Cells, 101, 36 (2012); https://doi.org/10.1016/j.solmat.2012.02.019

[70] M. Theelen, A. Liakopoulou, V. Hans, F. Daume, H. Steijvers, N. Barreau, Z. Vroon, M. Zeman, Journal of Renewable and Sustainable Energy, 9, 021205 (2017); https://doi.org/10.1063/1.4979963

[71] M. A. Rahman, Solar Energy, 215, 64 (2021); https://doi.org/10.1016/j.solener.2020.12.020